

ARTICLE

Synthetic, structural and reaction chemistry of N-heterocyclic germylene and stannylene compounds featuring N-boryl substituents

Received 00th January 20xx,
Accepted 00th January 20xx

DOI: 10.1039/x0xx00000x

Lilja Kristinsdóttir,^a Nicola L. Oldroyd,^a Rachel Grabiner,^a Alastair W. Knights,^a Andreas Heilmann,^a Andrey V. Protchenko,^a Haoyu Niu,^a Eugene L. Kolychev,^a Jesús Campos,^a Jamie Hicks,^a Kirsten E. Christensen^a and Simon Aldridge^{*a}

This study details the syntheses of N-heterocyclic germylenes and stannylenes featuring diazaborolyl groups, $\{(\text{HCDippN})_2\text{B}\}$ (Dipp = 2,6-*i*-Pr₂C₆H₃), as both of the N-bound substituents, with a view to generating electron rich and sterically protected metal centres. The energies of their key frontier orbitals – the group 14-centred lone pair and orthogonal p_π -orbital (typically the HOMO-2 and LUMO) have been probed by DFT calculations and compared with a related acyclic analogue, revealing (in the case of the stannylenes) a correlation with the measured ¹¹⁹Sn chemical shifts. The reactivity of the germylene systems towards oxygen atom transfer agents have been examined, with 2:1 reaction stoichiometries being observed for both Me₃NO and pyridine N-oxide, leading to the formation of products derived from the activation of C–H bonds by a transient first-formed germanone.

Introduction

The pioneering work of Lappert in the 1970s led to the development of persistent group 14 tetrelene compounds of the type EX₂, and an understanding that, while the lone pair at the tetrelene centre is nucleophilic, the formally empty p_π -orbital offers the possibility for complementary electrophilic behaviour.¹ It is this ambiphilic nature which has been exploited more recently in the activation of small molecules, such as H₂ and NH₃.² Key to facilitating such chemistry is the idea of minimizing the energetic separation between these orbitals (which often correspond to the HOMO and LUMO), by appropriate choice of the pendant X substituents.

We have recently exploited the bulky Dipp-substituted diazaborolyl group $\{(\text{HCDippN})_2\text{B}\}$ (Dipp = 2,6-*i*-Pr₂C₆H₃) as a strongly donating ancillary substituent to generate highly electron-rich main group complexes.^{3–5} The lithium reagent $\{(\text{HCDippN})_2\text{B}\}\text{Li}(\text{THF})_2$ ³ is, however, challenging to synthesize and is very sensitive to air and moisture. With this in mind, we have also been interested in using this boryl group as a more remote substituent within, for example, an amido or alkoxo framework, since such systems can typically be accessed from the more readily available bromoborane reagent $\{(\text{HCDippN})_2\}\text{BBr}$. Thus, for example, we recently reported the

synthesis of the acyclic silylenes, $\{(\text{HCDippN})_2\text{B}\}(\text{Me}_3\text{Si})\text{N}_2\text{Si}$ and $\{(\text{HCDippN})_2\text{B}\}\text{O}_2\text{Si}$, featuring boryl-derivatized amide and alkoxide donors, respectively (**I** and **II**, Figure 1).^{6,7} In addition, we have also recently reported transient N-heterocyclic carbenes (NHCs) featuring the diazaborolyl group, $\{(\text{HCDippN})_2\text{B}\}$, as one of the N-bound substituents.⁸

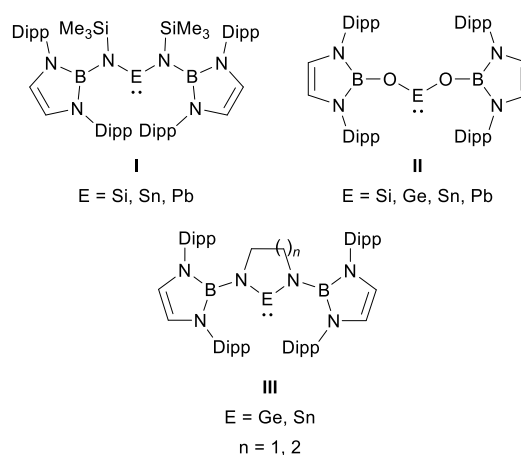


Figure 1. Previously reported tetrelenes bearing peripheral diazaborolyl substituents (**I** and **II**) and the systems targeted in the current study (**III**).

As an extension of this approach, we were interested to examine the use of this boryl group as the N-bound substituent in saturated N-heterocyclic germylenes and stannylenes (e.g. **III**, Figure 1). Compared to ‘regular’ amido substituents, the presence of the pendant boryl function would be expected to elevate the HOMO of the tetrelene (on account of their strong σ -donor capabilities), and potentially also lower the energy of

^a Inorganic Chemistry Laboratory, Department of Chemistry, University of Oxford, South Parks Road, Oxford, OX1 3QR, UK.
E-mail: simon.aldrige@chem.ox.ac.uk

Electronic Supplementary Information (ESI) available: additional synthetic details; details of DFT calculations; CIFs for X-ray crystal structures.
See DOI: 10.1039/x0xx00000x

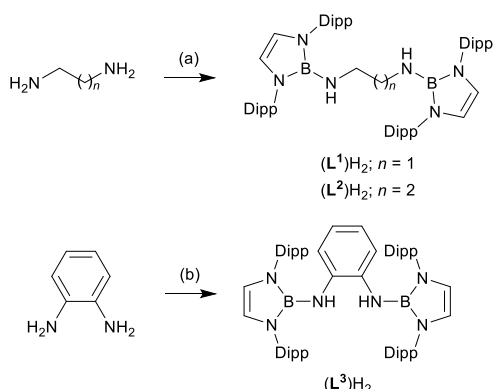
the LUMO, by reducing the N-to-E π -donor capabilities of the amido group. In addition, the presence of two bulky boryl N-substituents would be expected to generate very high peripheral steric loading in the vicinity of the germanium/tin centre which would not only hinder oligomerization, but might also offer a sterically protected 'pocket' in which to carry out further reaction chemistry.

In this manuscript we report on the syntheses of saturated N-heterocyclic germylenes and stannylenes featuring the diazaborolyl group as the N-bound substituents, and an exploration of the reactivity of such systems towards oxygen atom transfer reagents.

Results and discussion

Syntheses of N,N'-bisborylated diamine protio-ligands

Synthetically, the saturated N-heterocyclic tetrelenes were targeted from the respective bisborylated diamine protio-ligands, based on 1,2-diaminoethane and 1,3-diaminopropane backbones (Scheme 1). The N,N'-bisborylated protio-ligands (L^1)H₂ and (L^2)H₂, were synthesized *via* the reactions of the readily available bromoborane {(HCDippN)₂}BBr,^{3a,9} with 1,2-diaminoethane and 1,3-diaminopropane, respectively. Triethylamine was used to sequester the generated HBr, with (L^1)H₂ and (L^2)H₂ being isolated in yields of 81% and 93%, respectively (Scheme 1). Both compounds were characterized by standard spectroscopic/analytical techniques, and their structures in the solid state confirmed by X-ray crystallography (Figure 2). Spectroscopically, both (L^1)H₂ and (L^2)H₂ are characterized by ¹¹B NMR signals in the region expected for a boron centre bound to three nitrogen substituents (22–23 ppm); the observation of one backbone CH₂ signal for (L^1)H₂ and two signals (in a 2:1 ratio) for (L^2)H₂ in the respective ¹H NMR spectra is consistent with the formation of a symmetrical, bisborylated ligand skeleton.



Scheme 1. Syntheses of the bisborylated protio-ligands (L^1)H₂, (L^2)H₂ and (L^3)H₂. Reagents and conditions: (a) {(HCDippN)₂}BBr (2.0 equiv.), Et₃N, benzene, room temperature, 1–3 h, 81–93%; (b) {(HCDippN)₂}BBr (2.0 equiv.), Et₃N, benzene, 80 °C, 11 d, 62%.

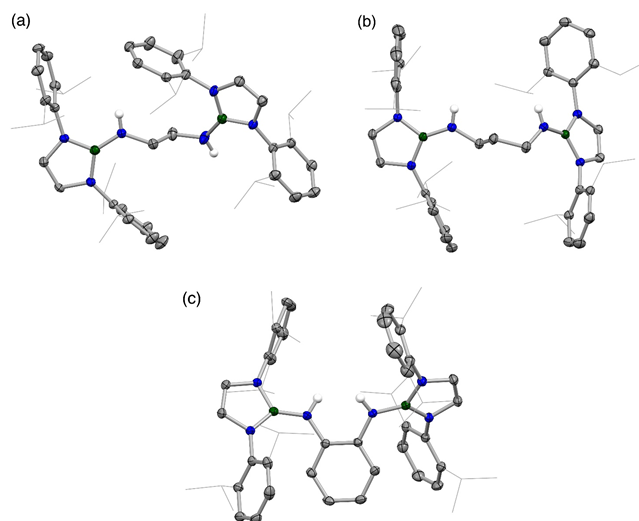
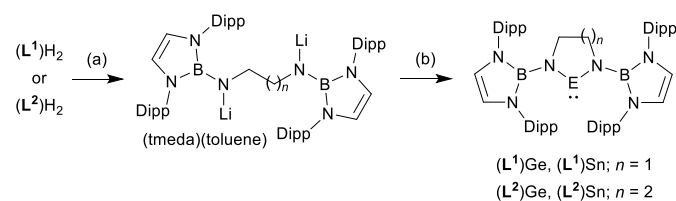


Figure 2. Molecular structures of (a) (L^1)H₂; (b) (L^2)H₂; and (c) (L^3)H₂ in the solid state as determined by X-ray crystallography. Most hydrogen atoms omitted and Dipp groups shown in wireframe format for clarity. Thermal ellipsoids set at the 35 % probability level. Key: boron, green; nitrogen, blue; carbon, grey; hydrogen, white. Key bond lengths (Å): (for (L^1)H₂): B–N(H) 1.413(5), 1.450(6); (for (L^2)H₂): B–N(H) 1.406(2), 1.411(2); (for (L^3)H₂): B–N(H) 1.433(2), 1.437(2).

The corresponding bisborylated protio-ligand based on an *ortho*-phenylene backbone, (L^3)H₂, can be synthesized in similar fashion *via* the reaction of {(HCDippN)₂}BBr with *ortho*-phenylenediamine. The more geometrically rigid nature of the backbone, however, makes the borylation chemistry considerably less facile. Thus, after *ca.* 1 day at 60 °C in the presence of 2 equivalents of {(HCDippN)₂}BBr, the ¹H NMR spectrum shows that half of the bromoborane remains unreacted, and an unsymmetrical new species was formed – assumed to be the mono-borylated diamine. Only on further heating (at 80 °C for 11 d) did full conversion occur to generate a symmetrical new species, which could be isolated as a pale yellow powder in 62% yield, and shown by spectroscopic and crystallographic techniques to be the bisborylated protio-ligand (L^3)H₂.

The ¹¹B shift of (L^3)H₂ (21 ppm) is very similar to those of (L^1)H₂ and (L^2)H₂, and crystallization from pentane at –20 °C yielded colourless crystals suitable for X-ray crystallography. It is clear from the molecular structure in the solid state (Figure 2) that the protio-ligand is very sterically crowded, reflecting the *cis*



Scheme 2. Syntheses of N,N'-bisborylated N-heterocyclic germylenes and stannylenes. Reagents and conditions: (a) ^tBuLi (4.0 eq.), TMEDA (1.0 equiv.), toluene, –50 °C to room temperature, 30 min.; (b) for (L^1)Ge and (L^2)Ge: GeCl₂:dioxane, room temperature, 16 h, 51% and 40%, respectively; for (L^1)Sn: SnCl₂, 80 °C, 24 h, 75% by NMR spectroscopy; for (L^2)Sn: SnCl₂, room temperature, 24 h, 35%.

disposition of the borylamine groups about the central C–C bond (C(1)–C(2)).

Syntheses of germynes and stannylenes

With the syntheses of the respective protio-ligands in hand, two methodologies were investigated for their subsequent conversion to the corresponding tetrelenes: (i) direct reaction with the respective bis(trimethylsilyl)amido derivatives, $E\{N(\text{SiMe}_3)_2\}_2$ ($E = \text{Ge}, \text{Sn}$); and (ii) deprotonation *via* reaction with an alkyllithium or -potassium base followed by metathesis with a germanium or tin dihalide. The former approach did not lead to any conversion even at elevated temperatures (*ca.* 110 °C). On the other hand, the use of excess (four equivalents) of $n\text{BuLi}$ in the presence of one equivalent of tetramethylethylenediamine (TMEDA) in toluene resulted in full consumption of the amine to yield the corresponding dilithioamide (as determined by ^1H NMR monitoring). Alternatively, the use of two equivalents of benzyl potassium in C_6D_6 generated the analogous dipotassium salt in quantitative yield. The lithium salts of both $[\text{L}^1]^{2-}$ and $[\text{L}^2]^{2-}$ could be characterized by multinuclear NMR as the mono-TMEDA, mono-toluene adducts, but single crystals suitable for X-ray crystallography could not be obtained. The germylene and stannylene systems (L^1Ge , L^2Ge , L^1Sn and L^2Sn) were then synthesized from the corresponding dilithio- or dipotassium amides by the addition of $\text{GeCl}_2\cdot\text{dioxane}$ or SnCl_2 , respectively, and characterized by standard spectroscopic methods and X-ray crystallography (Scheme 2 and Figure 3). The use of excess $n\text{BuLi}$ in the presence of TMEDA (*cf.* benzyl potassium) resulted in considerably lower contamination of the crude tetrelene products with the corresponding protio-ligands and ultimately to higher overall yields. Due to the high solubilities in compatible media, the isolated yields (35–51%) were typically somewhat lower than the percentage conversions implied by *in situ* ^1H NMR monitoring. Attempts to generate the corresponding systems featuring the phenylene-based ligand L^3 resulted in extremely facile decomposition and isolation instead of the protio-ligand $(\text{L}^3)\text{H}_2$.

For each tetrelene system, the observation of a single resonance in the ^1H NMR spectrum for the backbone CH groups of the boryl heterocycle, together with signals for the ^iPr groups (two doublets, one septet) consistent with the presence of only one such environment, are consistent with effective C_{2v} symmetry at the germanium/tin centre on the NMR timescale. In the case of the tin compounds (L^1Sn and L^2Sn), signals are observed at $\delta_{\text{Sn}} = 528$ and 458 ppm in the respective ^{119}Sn NMR spectra. Single crystals suitable for X-ray crystallography could be obtained for each of (L^1Ge , L^2Ge , L^1Sn and L^2Sn), although in the case of (L^1Sn co-crystallization with the protio-ligand $(\text{L}^1)\text{H}_2$ invariably occurs, making the isolation of bulk samples of the pure stannylene very difficult. For all four systems, the E–N bond lengths (1.854(1)/1.865(1) Å for (L^1Ge , 1.846(1)/1.866(1) Å for (L^2Ge , 2.073(4)/2.085(4) Å for (L^1Sn and 2.063(4)/2.086(5) Å for (L^2Sn) are within the sum of the respective covalent radii (1.91(5) Å for Ge–N and 2.10(5) Å for Sn–N),¹⁰ consistent with

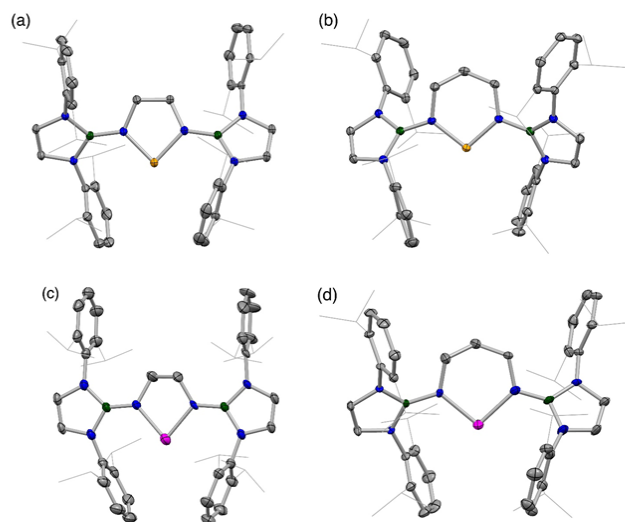


Figure 3. Molecular structures of (a) (L^1Ge); (b) (L^2Ge); (c) (L^1Sn); and (d) (L^2Sn) in the solid state as determined by X-ray crystallography. Hydrogen atoms, solvate molecules and second disorder component for (L^1Sn) omitted, and Dipp groups shown in wireframe format for clarity; thermal ellipsoids set at the 35% probability level. Key: germanium, orange; tin, pink; boron, green; nitrogen, blue; carbon, grey. Key bond lengths (Å), angles (°) and torsions (°): (for (L^1Ge): Ge–N 1.854(1), 1.865(1), B–N(Ge) 1.434(2), 1.436(2), N–Ge–N 88.0(1), N–B–N–Ge 31.1(2), 27.8(2); (for (L^2Ge): Ge–N 1.846(1), 1.866(1), B–N(Ge) 1.443(2), 1.444(2), N–Ge–N 99.8(1), N–B–N–Ge 33.9(2), 47.6(2); (for (L^1Sn): Sn–N 2.073(4), 2.085(4), B–N(Sn) 1.408(7), 1.419(7), N–Sn–N 82.5(2), N–B–N–Sn 5.2(8), 10.6(8); (for (L^2Sn): Sn–N 2.063(4), 2.086(5), B–N(Sn) 1.436(6), 1.445(5), N–Sn–N 96.8(2), N–B–N–Sn 33.0(5), 41.1(6).

descriptions as essentially single covalent Ge–N and Sn–N bonds. As expected, the N–Ge–N angle widens significantly on lengthening the backbone (88.0(1)° for (L^1Ge ; 99.8(1)° for (L^2Ge). For a given ligand backbone, the N–Sn–N angle is more acute than its germylene analogue (*e.g.* (L^2Ge : 99.8(1)°; (L^2Sn : 96.8(2)°), in line with the reduced degree of *s/p* mixing expected on descending group 14. More generally, the N–Sn–N angles in (L^1Sn and (L^2Sn (82.5(2) and 96.8(2)°) are significantly more acute than those found in related acyclic analogues such as $\{(\text{HCDippN})_2\text{B}\}^t\text{BuN}\}_2\text{Sn}$ ($(\text{L}^4)_2\text{Sn}$, 106.9(1)° – see ESI) and $\{(\text{HCDippN})_2\text{B}\}(\text{Me}_3\text{Si})\text{N}\}_2\text{Sn}$ (106.13°).^{6a} Interestingly, in the solid state, the diazaborolyl heterocycles in (L^1Ge , (L^2Ge and (L^2Sn do not lie co-planar with the tetrelene heterocycle (being twisted at angles of between 27.8(2) and 47.6(2)°) implying that the presence of the boryl group is not likely to affect the energy of the germanium- or tin-centred LUMO to any great degree. In the case of (L^1Sn , however, the corresponding torsion angles are much smaller (*ca.* 5–10°) implying that N-to-B π -donation might compete with N-to-Sn π -donation.

DFT calculations

The energies of the frontier orbitals of (L^1E and (L^2E , as well as the related bis(monodentate) systems, $(\text{L}^4)_2\text{E}$, have been calculated by DFT methods for both $E = \text{Ge}$ and Sn , together with those for the corresponding (model) silylene compounds (*i.e.* $E = \text{Si}$). The results are shown in Table 1. In each case, the HOMO-2 has significant lone pair character at the tetrelene centre, and the formally empty p_π -orbital centred at E is the LUMO. The

HOMO and HOMO-1 are associated with the π -systems of the boryl groups and the amido nitrogens.

Upon descending Group 14, the angle at the tetrelene centre decreases, in line with the expected decrease in valence s/p mixing with increasing atomic number. Energetically, for all three ligand systems (L^1 , L^2 and L^4), the largest change on going from E = Si to Ge to Sn can be seen in the energy of LUMO, which is lower in energy for the heavier tetrelenes. This trend runs contrary to that expected on the basis of the energies of the valence np orbitals ($n = 3 - 5$), and can be rationalized on the basis of the decreasing extent of N-to-E π -donation. π -Overlap between the α -nitrogens and E is greatest for E = Si; for the heavier elements, germanium, and particularly tin, N-E π -overlap is much poorer and the LUMO (which has N-E π^* character) is not destabilized to the same degree. The energies of the E-centred lone pair (the HOMO-2) are less affected as E changes, being stabilized by *ca.* 20–30 kJ mol⁻¹ for Sn, relative to Si, as expected on the basis of increasing *ns* (vs. *np*) character as the N-E-N angle narrows. The much larger decrease in the LUMO energies therefore underpins why the (HOMO-2)-LUMO gap (ΔE) actually decreases for each ligand on going from E = Si to Sn.

Tetrelene	E	N-E-N Angle (°)	HOMO-2 (kJ mol ⁻¹)	LUMO (kJ mol ⁻¹)	ΔE
$(L^1)E$	Si	91	-502	-171	331
	Ge	87	-533	-204	329
	Sn	81	-535	-231	304
$(L^2)E$	Si	102	-497	-139	358
	Ge	100	-527	-185	342
	Sn	95	-530	-218	312
$(L^4)_2E$	Si	121	-436	-107	329
	Ge	113	-441	-200	241
	Sn	112	-473	-266	207

Table 1. DFT-calculated geometric and electronic parameters for cyclic and acyclic tetrelene systems, $(L^1)E$, $(L^2)E$ and $(L^4)_2E$ (E = Si, Ge, Sn).

Comparing between ligand systems it can be seen that ΔE for the cyclic tetrelenes is greater than for their acyclic analogues, implying lower levels of reactivity. The narrower N-E-N bond angles for $(L^1)E$ and $(L^2)E$ compared with the corresponding acyclic systems $(L^4)_2E$ are reflected in the lower energy of the HOMO-2 (greater *ns* character), and is the primary reason for the larger values of ΔE .¹¹ Moreover, these data are in line with the measured ¹¹⁹Sn chemical shifts for the stannylene systems, with the smaller energetic separation (ΔE) for the acyclic system being associated with a more downfield shifted resonance:¹² $(L^4)_2E$: $\delta_{Sn} = 644$ ppm ($\Delta E = 207$ kJ mol⁻¹) vs $(L^1)Sn$: $\delta_{Sn} = 528$ ppm ($\Delta E = 304$ kJ mol⁻¹) and $(L^2)Sn$: $\delta_{Sn} = 458$ ppm ($\Delta E = 312$ kJ mol⁻¹).

Counter-intuitively, however, the ¹¹⁹Sn chemical shift for $(L^2)Sn$ is at higher field (and ΔE is larger) than for $(L^1)Sn$, despite the wider angle at the tin centre enforced by larger six-membered heterocycle (95° vs 81° (calc.)). This reflects differences in the destabilization of the LUMO, which in turn have geometric

origins. In the case of $(L^1)Sn$, the pendant boryl heterocycles lie essentially co-planar with the central SnN_2C_2 ring, allowing for competing π -interaction of the α -nitrogens with the three-coordinate boron centres, and consequently less effective interaction with the Sn-centred p_z -orbital (Figure 4). In the case of $(L^2)Sn$, the extra backbone CH_2 group forces the boryl substituents closer together in space, causing them to rotate out of plane (torsion angles of *ca.* 34°), and thereby reduce the extent of competing N-to-B π -donation. As such, the LUMO in $(L^2)Sn$ is somewhat more destabilized than that in $(L^1)Sn$.

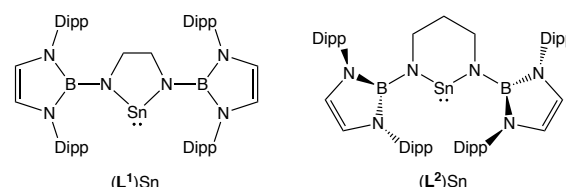


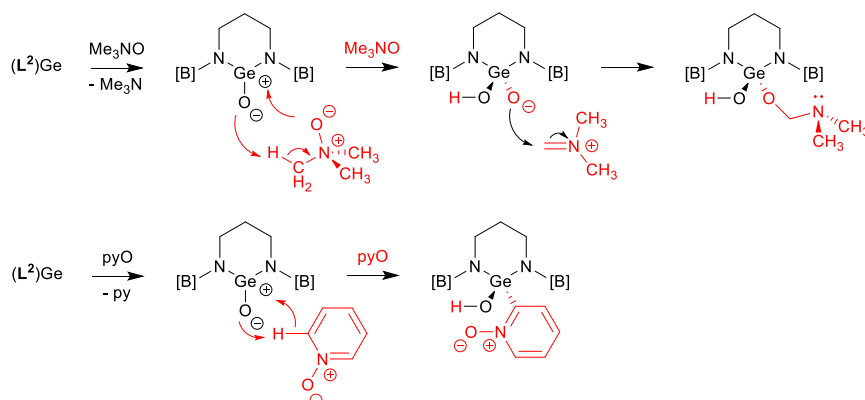
Figure 4. Differing conformational alignments of the pendant boryl heterocycles in $(L^1)Sn$ and $(L^2)Sn$.

Reactivity studies

The reactivity of the new tetrelene compounds towards a range of small molecules has been investigated. These studies centred on the germylene systems, given their easier purification, and our recent focus on understanding the factors underpinning reactivity in such compounds.^{13,14} In particular, we targeted exploration of the chemistry of $(L^2)Ge$, given the very high degree of shielding in the vicinity of the metal centre in this compound, and the potential for generating reactive Ge-X bonds within a sterically shrouded 'pocket'.¹⁵ We also perceived that the strong pendant B-N bonds would also provide a significant barrier to rearrangement processes leading to migration of the boryl substituents.⁸ With this in mind, attention focussed on reactivity towards O-atom (and related) transfer agents, with the particular aim of generating a germanone functionality within the sterically protected coordination environment of $(L^2)Ge$.

In contrast to ketones (which usually exist in monomeric form), their heavier analogues show a much greater tendency to oligomerize or polymerize.¹⁶ Upon descending Group 14, the E=O π -bond becomes intrinsically weaker and more polar, due to less effective $p\pi$ -overlap and greater differences in electronegativity.^{16a} To date, only a few example of stable unsupported silanones, germanones and stannones have been isolated (*i.e.* ones not additionally stabilized by an electron-donating Lewis base or a transition metal fragment), and these typically feature very bulky supporting ligand sets.¹⁷

The reactivity of a range of oxygen-atom transfer agents was investigated with $(L^2)Ge$. Of these N_2O , CO_2 , O_2 , lutidine N-oxide and 2,6-dichloropyridine N-oxide showed no reactivity. Conversion to new products was observed, however, in the cases of Me_3NO and pyridine N-oxide. The ¹H NMR spectrum of a reaction mixture comprised of equimolar amounts of Me_3NO and $(L^2)Ge$ shows that 50% of the germylene remains



Scheme 3. Proposed mechanisms for the reactions of (L²)Ge with Me₃NO (upper) and pyridine N-oxide (lower).²⁸

unreacted after 3 h at room temperature; upon addition of a further equivalent of Me₃NO, the reaction proceeds to completion. This new product is characterized by two overlapping septets for the isopropyl CH units and four doublets for the corresponding CH₃ groups, implying a lower symmetry at the metal centre than in the parent germylene. Single crystals suitable for X-ray crystallography could be obtained by slow evaporation of a cyclohexane solution. The solid-state structure so obtained (Figure 5) features a four-coordinate germanium centre bearing additional OCH₂NMe₂ and OH ligands (*i.e.* (L²)Ge(OCH₂NMe₂)(OH)).

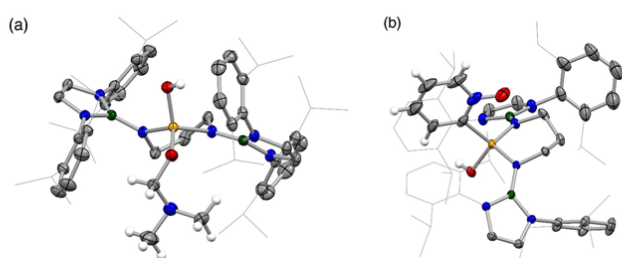


Figure 5. Molecular structures of (a) (L²)Ge(OCH₂NMe₂)(OH); and (b) (L²)Ge(C₅H₄NO)(OH) in the solid state as determined by X-ray crystallography. Most hydrogen atoms omitted, and Dipp groups shown in wireframe format for clarity; thermal ellipsoids set at the 40% probability level. Key: germanium, orange; tin, pink; boron, green; nitrogen, blue; carbon, grey; hydrogen, white. Key bond lengths (Å) and angles (°): (for (L²)Ge(OCH₂NMe₂)(OH)): Ge–N 1.809(2), 1.822(2), B–N(Ge) 1.435(3), 1.444(3), Ge–O(H) 1.761(2), Ge–O 1.764(2), N–Ge–N 103.4(1); (for (L²)Ge(C₅H₄NO)(OH)): Ge–N 1.810(2), 1.833(2), B–N(Ge) 1.432(3), 1.435(3), Ge–O(H) 1.765(2), Ge–C 1.955(3), N–Ge–N 107.1(1).

Related chemistry has been reported by Veith *et al.*,¹⁸ who suggest that a similar reaction proceeds through a transient germanone which then reacts with a second equivalent of Me₃NO. A mechanism is therefore proposed for the reaction of (L²)Ge with Me₃NO (Scheme 3) that reflects the need for two equivalents of the amine oxide to drive the reaction to completion. Initial germanone formation is followed by coordination of a second molecule of Me₃NO at the highly electrophilic germanium centre and proton transfer to the basic germanone oxygen (Scheme 3). Ejection of an iminium fragment then reassimilation in the opposite sense *via* C–O

bond formation then accounts for the formation of the observed product.

In the case of pyridine N-oxide, the reaction requires heating to 110 °C and the use of two equivalents to proceed to completion; the ¹H NMR spectrum of the product suggests a lowering of symmetry at germanium similar to that observed in the reaction with Me₃NO. Single crystals suitable for X-ray crystallography were obtained by recrystallization from hexane, and the solid-state structure obtained (Figure 5) also reveals a Ge(IV) compound, in this case featuring featuring OH and C₅H₄NO ligands in addition to L². The formation of (L²)Ge(C₅H₄NO)(OH) presumably follows a pathway similar to the reaction with Me₃NO, *i.e.* *via* a transient germanone, which then activates (deprotonates) the ortho C–H bond of a second pyridine N-oxide molecule across the highly reactive Ge=O unit.

Conclusions

We have synthesized N-heterocyclic tetrelenes featuring the diazaborolyl group, {(HCNDipp)₂B}, as the N-bound substituents, in order to generate strongly electron-donating and sterically imposing coordination environments at the respective metal centres. Structural characterization by X-ray crystallography has proved possible in the cases of (L¹)Ge, (L²)Ge, (L¹)Sn and (L²)Sn, and DFT calculations offer comparison of key orbital energies with related acyclic systems. The reactivity of (L²)Ge towards oxygen transfer agents has been explored: initially formed germanone species appear to be extremely reactive, with facile activation of a second molecule of Me₃NO or pyridine N-oxide being observed irrespective of reaction stoichiometry. Efforts towards the synthesis of heavier ketone analogues bearing other boryl-functionalized ligands are currently ongoing, specifically targeting systems which are reactive towards the more ‘innocent’ O-atom source N₂O.

Experimental section

General methods and instrumentation

All manipulations were carried out using standard Schlenk line and glove box techniques under an atmosphere of argon and dinitrogen, respectively. With the exceptions of tetrahydrofuran, cyclohexane and diethyl ether, solvents were dried using a commercially available Braun SPS,¹⁹ purged with argon and stored over potassium mirror in a J. Young's ampoule. Tetrahydrofuran, cyclohexane and diethyl ether were distilled from sodium/benzophenone. C₆D₆ and toluene-d₈ were dried over CaH₂ (overnight), distilled, stored over potassium mirror in a J. Young's ampoule and degassed by three freeze-pump-thaw cycles. Triethylamine, 1,2-diamino-ethane, 1,3-diaminopropane, ⁿBuLi (stored in a J. Young's ampoule) and GeCl₂-dioxane (stored in a glove box) were used as received. TMEDA was dried over sodium wire, SnCl₂ and trimethylamine N-oxide were sublimed *in vacuo* at 170 °C and 120 °C, respectively. Pyridine N-oxide was dried over P₂O₅ and sublimed *in vacuo* at room temperature. Lutidine N-oxide was dried over activated sieves in C₆D₆. {(HCDippN)₂}BBr⁹ and benzyl potassium²⁰ were synthesized according to literature procedures. ¹H, ⁷Li, ¹¹B, ¹³C{¹H}, ¹⁹F, ²⁹Si and ¹¹⁷Sn NMR spectra were measured on a Bruker Avance III HD nanobay 400 MHz or a Bruker AVC500 spectrometer and referenced internally to residual protio-solvent (¹H) or solvent (¹³C) resonances, and are reported relative to tetramethylsilane ($\delta = 0$ ppm). ¹¹B and ¹⁹F NMR spectra were referenced to external Et₂O·BF₃, and ⁷Li, ²⁹Si and ¹¹⁷Sn to 1 M LiCl in D₂O, SiMe₄ and SnMe₄ in C₆D₆, respectively. Assignments were confirmed using two dimensional ¹H-¹H and ¹³C-¹H NMR correlation experiments. Chemical shifts are quoted in δ (ppm) and coupling constants in Hz. Elemental analyses were carried out by London Metropolitan University.

Syntheses of novel compounds

(L¹)H₂: 1,2-diaminoethane (0.22 mL, 3.2 mmol) was dissolved in triethylamine (3 mL) and the resulting solution added to a solution of {(HCDippN)₂}BBr (3.0 g, 6.4 mmol) in benzene (15 mL). The resulting orange mixture was stirred at room temperature for 1 h, whereupon a white precipitate formed immediately. After filtration, volatiles were removed *in vacuo*, and the residue washed with acetonitrile (3 x 10 mL) and dried *in vacuo*, yielding (L¹)H₂ as a white powder. Yield: 2.2 g, 81%. Colourless crystals suitable for X-ray crystallography could be obtained by recrystallization from a pentane solution at -20 °C. ¹H NMR (C₆D₆, 400 MHz, 298 K): δ_{H} 6.96-7.12 (12H, overlapping m, *m*-H and *p*-H of Dipp), 5.99 (s, 4H, N(CH₂)₂N of boryl ligand), 3.30 (8H, sept, ³J_{HH} = 6.9 Hz, CHMe₂), 2.27 (4H, m, NCH₂), 1.43 (2H, t, ³J_{HH} = 7.2 Hz, NH), 1.19 (24H, d, ³J_{HH} = 6.9 Hz, CHMe₂), 1.15 (24H, d, ³J_{HH} = 6.9 Hz, CHMe₂). ¹³C{¹H} NMR (C₆D₆, 101 MHz, 298 K): δ_{C} 147.1 (*o*-C of Dipp), 139.0 (*i*-C of Dipp), 127.5 (*p*-C of Dipp), 123.7 (*m*-C of Dipp), 117.4 (N(CH₂)₂N of boryl ligand), 45.0 (NCH₂), 28.5 (CHMe₂), 24.8 (CHMe₂), 23.7 (CHMe₂). ¹¹B NMR (C₆D₆, 128 MHz, 298 K): δ_{B} 23 (br s, boryl ligand). MS (CI): *m/z* (assignment, %) 833.7 ([M]⁺, 20%). Acc. Mass ESI: calc. for [C₅₄H₇₉¹⁰B₂N₆]⁺: 831.6625; found: 831.6615.

(L²)H₂: (L²)H₂ was synthesized by a similar method to (L¹)H₂ from 1,3-diaminopropane (0.18 mL, 2.1 mmol), triethylamine (2 mL) and {(HCDippN)₂}BBr (2.0 g, 4.3 mmol). The solution was stirred for 3 h and (L²)H₂ obtained as a white powder. Yield: 1.7 g, 93%. Colourless crystals suitable for X-ray crystallography could be obtained by recrystallization from a hexane solution at -20 °C. ¹H NMR (C₆D₆, 400 MHz, 298 K): δ_{H} 7.11-7.24 (overlapping m, *p*-H and *m*-H of Dipp and C₆D₅H), 5.88 (4H, s, N(CH₂)₂N of boryl ligand), 3.34 (8H, sept, ³J_{HH} = 6.9 Hz, CHMe₂), 2.07 (4H, dt, ³J_{HH} = 7.1 Hz, ³J_{HH} = 6.9 Hz, NCH₂), 1.23 (24H, d, ³J_{HH} = 6.9 Hz, CHMe₂), 1.17-1.19 (26H, overlapping m, CHMe₂, NH), 0.57 (2H, quint, ³J_{HH} = 7.1 Hz, CH₂(CH₂N)₂). Integration of *m*-H and *p*-H of Dipp is slightly higher than expected due to partial overlap with C₆D₅H. ¹³C{¹H} NMR (C₆D₆, 101 MHz, 298 K): δ_{C} 147.3 (*o*-C of Dipp), 139.3 (*i*-C of Dipp), 127.5 (*p*-C of Dipp), 123.6 (*m*-C of Dipp), 117.4 (N(CH₂)₂N of boryl ligand), 39.1 (NCH₂), 37.7 (CH₂(CH₂N)₂), 28.5 (CHMe₂), 24.6 (CHMe₂), 23.8 (CHMe₂). ¹¹B NMR (C₆D₆, 128 MHz, 298 K): δ_{B} 22 (br s, boryl ligand). MS (CI): *m/z* (assignment, %) 847.7 ([M]⁺, 0.3%). Acc. Mass ESI: calc. for [C₅₅H₈₁¹⁰B₂N₆]⁺: 845.6781; found: 845.6781. Elemental microanalysis: found (calcd. for C₅₅H₈₀B₂N₆): C 76.06 (76.53)%, H 9.42 (9.52)%, N 9.49 (9.92)%.

(L³)H₂: *ortho*-Phenylenediamine (58 mg, 0.53 mmol) and {(HCDippN)₂}BBr (0.50 g, 1.1 mmol) were dissolved in benzene (2.5 mL). Triethylamine (1 mL) was added to the solution and the resulting orange mixture stirred at 80 °C for 11 d, with a white precipitate gradually forming. Volatiles were removed *in vacuo* and the residue washed with acetonitrile (3 x 5 mL) and dried *in vacuo* yielding (L³)H₂ as a white powder (0.29 mg, 62% yield). Colourless crystals suitable for X-ray diffraction were obtained from pentane solution at -20 °C. ¹H NMR (C₆D₆, 400 MHz, 298 K): δ 7.13 (4H, m, *p*-Ar Dipp), 7.02 (8H, m, *m*-Ar Dipp), 6.51 (2H, m, ([B]NCCHCH)₂), 6.04 (2H, m, ([B]NCCHCH)₂), 5.98 (4H, s, NCH), 3.72 (2H, s, NH), 3.30 (8H, sept, ³J_{HH} = 6.8 Hz, CHMe₂), 1.18 (24H, d, ³J_{HH} = 6.8 Hz, CHMe₂), 1.02 (24H, d, ³J_{HH} = 6.8 Hz, CHMe₂); ¹³C NMR (C₆D₆, 101 MHz, 298 K): δ 146.2 (*o*-Ar Dipp), 139.2 (*i*-Ar Dipp), 132.4 ([B]NCCHCH)₂, 127.6 (*p*-Ar Dipp), 124.0 (*m*-Ar Dipp), 121.2 ([B]NCCHCH)₂, 120.2 ([B]NCCHCH)₂, 118.4 (NCH), 28.6 (CHMe₂), 25.0 (CHMe₂), 23.6 (CHMe₂); ¹¹B NMR (C₆D₆, 128 MHz, 298 K): δ 21. EI/MS: 882 ([M+H]⁺, 0.3%); accurate mass: calc. 879.6625, meas. 879.6638.

(L¹)Ge: To a stirred mixture of (L¹)H₂ (500 mg, 0.60 mmol) and TMEDA (90 μ L, 0.60 mmol) in toluene (10 mL) at -50 °C was added dropwise ⁿBuLi (1.6 mL of a 1.6 M solution in hexane, 2.5 mmol). The resulting orange reaction mixture was left to reach room temperature and stirred for a further 1 h. GeCl₂-dioxane (500 mg, 2.1 mmol) was subsequently added and the resulting reaction mixture stirred overnight, producing a yellow solution with a white precipitate. Volatiles were removed *in vacuo* and the product extracted into pentane and filtered. The filtrate was concentrated and the solution cooled to -20 °C to produce orange crystals. After filtration, the orange crystals were washed with cold pentane (-30 °C; 2 x 10 mL) and dried *in vacuo*. Yield: 280 mg, 51% yield. Yellow single crystals suitable for X-ray crystallography could be obtained by recrystallization from

pentane at $-20\text{ }^{\circ}\text{C}$. ^1H NMR (C_6D_6 , 400 MHz, 298 K): δ_{H} 6.01–7.16 (overlapping m, *p*-H and *m*-H of Dipp and $\text{C}_6\text{D}_5\text{H}$), 5.98 (4H, s, $\text{N}(\text{CH}_2)_2\text{N}$ of boryl ligand), 3.28 (8H, sept, $^3J_{\text{HH}} = 6.8\text{ Hz}$, CHMe_2), 2.93 (4H, s, NCH_2), 1.19 (24H, d, $^3J_{\text{HH}} = 6.8\text{ Hz}$, CHMe_2), 1.11 (24H, d, $^3J_{\text{HH}} = 6.8\text{ Hz}$, CHMe_2). Integration of *m*-H and *p*-H of Dipp is slightly higher than expected due to partial overlap with $\text{C}_6\text{D}_5\text{H}$. $^{13}\text{C}\{^1\text{H}\}$ NMR (C_6D_6 , 101 MHz, 298 K): δ_{C} 146.5 (*o*-C of Dipp), 140.1 (*i*-C of Dipp), 127.8 (*p*-C of Dipp), 124.0 (*m*-C of Dipp), 118.0 ($\text{N}(\text{CH}_2)_2\text{N}$ of boryl ligand), 51.3 (NCH_2), 28.6 (CHMe_2), 25.1 (CHMe_2), 23.4 (CHMe_2). ^{11}B NMR (C_6D_6 , 128 MHz, 298 K): δ_{B} 24 (br s, boryl ligand). Elemental microanalysis: found (calcd. for $\text{C}_{54}\text{H}_{76}\text{B}_2\text{N}_6\text{Ge}$): C 71.80 (71.79)%, H 8.69 (8.48)%, N 8.86 (9.30)%.

(L^2)Ge: (L^2)Ge was prepared from $\text{Li}_2(\text{L}^2)$ by a similar method to (L^1)Ge, using (L^2) H_2 (0.90 g, 1.1 mmol), TMEDA (160 μL , 1.1 mmol), $n\text{BuLi}$ (2.7 mL of a 1.6 M solution in hexane, 4.3 mmol) and $\text{GeCl}_2\cdot\text{dioxane}$ (0.87 mg, 3.7 mmol) in toluene (5 mL). The product was isolated by recrystallization from hexane at $-20\text{ }^{\circ}\text{C}$. Yield: 0.39 g, 40% yield. ^1H NMR (C_6D_6 , 400 MHz, 298 K): δ_{H} 7.04–7.20 (overlapping m, *p*-H and *m*-H of Dipp and $\text{C}_6\text{D}_5\text{H}$), 5.97 (4H, s, $\text{N}(\text{CH}_2)_2\text{N}$ of boryl ligand), 3.29 (8H, sept, $^3J_{\text{HH}} = 6.9\text{ Hz}$, CHMe_2), 2.80 (4H, m, NCH_2), 1.12–1.24 (50H, overlapping m, CHMe_2 and $\text{CH}_2(\text{NCH}_2)_2$). Integration of *m*-H and *p*-H of Dipp is slightly higher than expected due to partial overlap with $\text{C}_6\text{D}_5\text{H}$. $^{13}\text{C}\{^1\text{H}\}$ NMR (C_6D_6 , 101 MHz, 298 K): δ_{C} 146.0 (*o*-C of Dipp), 140.2 (*i*-C of Dipp), 127.5 (*p*-C of Dipp), 124.0 (*m*-C of Dipp), 118.6 ($\text{N}(\text{CH}_2)_2\text{N}$ of boryl ligand), 46.8 (NCH_2), 33.5 ($\text{CH}_2(\text{CH}_2\text{N})_2$), 28.7 (CHMe_2), 25.4 (CHMe_2), 23.8 (CHMe_2). ^{11}B NMR (C_6D_6 , 128 MHz, 298 K): δ_{B} 25 (br s, boryl group). MS (EI): m/z (assignment, %) 918.6 ($[\text{M}]^+$, 0.6%). Acc. Mass ESI: calc. for $[\text{C}_{55}\text{H}_{78}\text{B}_2\text{N}_6\text{Ge}]^+$: 918.5686; found: 918.5714.

(L^1)Sn: (L^1)Sn was prepared from $\text{Li}_2(\text{L}^1)$ by a similar method to (L^1)Ge using (L^1) H_2 (0.20 g, 0.24 mmol), TMEDA (36 μL , 0.24 mmol), $n\text{BuLi}$ (0.60 mL of a 1.6 M solution in hexane, 0.96 mmol) and SnCl_2 (46 mg, 0.24 mmol) in toluene (2 mL). After the addition of SnCl_2 , the reaction mixture was stirred at $80\text{ }^{\circ}\text{C}$ for 24 h. The hexane filtrate was slowly concentrated to yield a small quantity of orange crystals suitable for X-ray crystallography. The product could not be crystallized for isolation on a bulk scale due to high solubility, moisture sensitivity and contamination of (L^1) H_2 . Samples are invariably contaminated with ca. 25% of (L^1) H_2 . ^1H NMR (C_6D_6 , 400 MHz, 298 K): δ_{H} 7.01–7.13 (overlapping m, *m*-C and *p*-C of Dipp), 5.99 (4H, s, $\text{N}(\text{CH}_2)_2\text{N}$ of boryl ligand), 3.35 (8H, sept, $^3J_{\text{HH}} = 6.8\text{ Hz}$, CHMe_2), 3.07 (4H, s, NCH_2), 1.19 (24H, d, $^3J_{\text{HH}} = 6.8\text{ Hz}$, CHMe_2), 1.15 (24H, d, $^3J_{\text{HH}} = 6.8\text{ Hz}$, CHMe_2). ^{11}B NMR (C_6D_6 , 128 MHz, 298 K): δ_{B} 24 (br s, boryl ligand). ^{119}Sn NMR (C_6D_6 , 149 MHz, 298 K): δ_{Sn} 527–529 (br s).

(L^2)Sn: (L^2)Sn was prepared in a similar method to (L^1)Ge, using (L^2) H_2 (0.50 g, 0.59 mmol), TMEDA (90 μL , 0.59 mmol), $n\text{BuLi}$ (1.5 mL of a 1.6 M solution in hexane, 2.5 mmol) and SnCl_2 (0.39 mg, 2.1 mmol) in toluene (4 mL). After the addition of SnCl_2 , the reaction mixture was stirred at room temperature for 24 h. Yield: 0.20 g, 35%. Orange single crystals suitable for X-ray

crystallography could be obtained by recrystallization from pentane at $-20\text{ }^{\circ}\text{C}$. Samples are invariably contaminated with ca. 15% of (L^2) H_2 . ^1H NMR (C_6D_6 , 400 MHz, 298 K): δ_{H} 7.05–7.22 (12H, overlapping m, *p*-H and *m*-H of Dipp and $\text{C}_6\text{D}_5\text{H}$), 5.97 (4H, s, $\text{N}(\text{CH}_2)_2\text{N}$ of boryl ligand), 3.36 (8H, sept, $^3J_{\text{HH}} = 6.9\text{ Hz}$, CHMe_2), 3.05 (4H, dd, $^3J_{\text{HH}} = 7.1\text{ Hz}$, $^3J_{\text{HH}} = 6.9\text{ Hz}$, NCH_2), 1.18–1.25 (50H, overlapping m, CHMe_2 and $\text{CH}_2(\text{CH}_2\text{N})_2$). Integration of *m*-H and *p*-H of Dipp is slightly higher than expected due to partial overlap with $\text{C}_6\text{D}_5\text{H}$. $^{13}\text{C}\{^1\text{H}\}$ NMR (C_6D_6 , 101 MHz, 298 K): δ_{C} 146.5 (*o*-C of Dipp), 140.7 (*i*-C of Dipp), 127.7 (*p*-C of Dipp), 124.2 (*m*-C of Dipp), 118.3 ($\text{N}(\text{CH}_2)_2\text{N}$ of boryl ligand), 47.6 (NCH_2), 37.7 ($\text{CH}_2(\text{CH}_2\text{N})_2$), 28.6 (CHMe_2), 25.4 (CHMe_2), 23.6 (CHMe_2). ^{11}B NMR (C_6D_6 , 128 MHz, 298 K): δ_{B} 25 (br s, boryl ligand). ^{119}Sn NMR (C_6D_6 , 149 MHz, 298 K): δ_{Sn} 457–459 (br s). MS (EI): m/z (assignment, %) 964.6 ($[\text{M}]^+$, 0.6%). Acc. Mass ESI: calc. for $[\text{C}_{55}\text{H}_{78}\text{B}_2\text{N}_6\text{Ge}]^+$: 964.5496; found: 964.5557.

(L^2)Ge(OCH_2NMe_2)(OH): A mixture of (L^2)Ge (36 mg, 0.04 mmol) and trimethylamine *N*-oxide (6 mg, 0.08 mmol) in a J. Young's NMR tube was dissolved in C_6D_6 and the resulting solution sonicated for 3 h, at which point it had turned pale yellow. Single crystals suitable for X-ray crystallography could be obtained by recrystallization from cyclohexane at $-20\text{ }^{\circ}\text{C}$. The remainder of the crystals were isolated for characterization by filtration of the supernatant but are invariably contaminated with ca. 7% of germanediol, (L^2)Ge(OH) $_2$. ^1H NMR (C_6D_6 , 400 MHz, 298 K): δ_{H} 7.10–7.20 (12H, overlapping m, *m*-H and *p*-H of Dipp), 5.92 (4H, s, $\text{N}(\text{CH}_2)_2\text{N}$ of boryl ligand), 3.45 (2H, s, OCH_2), 3.31–3.44 (8H, overlapping sept, CHMe_2), 2.89 (4H, m, NCH_2), 2.20 (6H, s, NMe_2), 1.17 (12H, d, $^3J_{\text{HH}} = 6.7\text{ Hz}$, CHMe_2), 1.20 (12H, d, $^3J_{\text{HH}} = 6.7\text{ Hz}$, CHMe_2), 1.30 (12H, d, $^3J_{\text{HH}} = 6.7\text{ Hz}$, CHMe_2), 1.35 (12H, d, $^3J_{\text{HH}} = 6.7\text{ Hz}$, CHMe_2), 0.85–0.67 (2H, m, $\text{CH}_2(\text{CH}_2\text{N})_2$), 0.24 (1H, s, OH). $^{13}\text{C}\{^1\text{H}\}$ NMR (C_6D_6 , 101 MHz, 298 K): δ_{C} 147.1 (*o*-C of Dipp), 147.0 (*o*-C of Dipp), 140.4 (*i*-C of Dipp), 127.6 (*p*-C of Dipp), 123.8 (*m*-C of Dipp), 123.7 (*m*-C of Dipp), 119.1 ($\text{N}(\text{CH}_2)_2\text{N}$ of boryl ligand), 82.9 (OCH_2), 47.3 (NCH_2), 41.7 (NMe_2), 31.5 ($\text{CH}_2(\text{CH}_2\text{N})_2$), 28.6 (CHMe_2), 28.5 (CHMe_2), 26.3 (CHMe_2), 26.3 (CHMe_2), 23.7 (CHMe_2), 23.5 (CHMe_2). ^{11}B NMR (C_6D_6 , 128 MHz, 298 K): δ_{B} 24 (br s, boryl ligand).

(L^2)Ge($\text{C}_5\text{H}_4\text{NO}$)(OH): (L^2)Ge($\text{C}_5\text{H}_4\text{NO}$)(OH) was prepared in a similar method to (L^1)Ge($\text{C}_5\text{H}_4\text{NO}$)(OH) using (L^2)Ge (23 mg, 0.025 mmol) and pyridine *N*-oxide (5 mg, 0.05 mmol) in toluene- d_8 (0.5 mL). Single crystals suitable for X-ray crystallography were grown from a hexane solution at $-20\text{ }^{\circ}\text{C}$. The remainder of the crystals were isolated for characterization by filtration of the supernatant but are invariably contaminated with ca. 5% of germanediol, (L^2)Ge(OH) $_2$. ^1H NMR (toluene- d_8 , 400 MHz, 298 K): δ_{H} 6.81–7.24 (overlapping m, *p*-H and *m*-H of Dipp and toluene- d_8), 7.45 (1H, m, $\text{Ge}\{\text{C}(\text{CH})_3\text{CH}(\text{NO})\}$), 6.14 (2H, overlapping m, $\text{Ge}\{\text{CCH}(\text{CH})_3(\text{NO})\}$ and $\text{Ge}\{\text{C}(\text{CH}_2)_2\text{CH}(\text{NO})\}$), 5.90 (4H, s, $\text{N}(\text{CH}_2)_2\text{N}$ of boryl ligand), 5.64 (1H, m, $\text{Ge}\{\text{CCHCH}(\text{CH})_2(\text{NO})\}$), 3.41 (8H, overlapping m, CHMe_2), 3.80 (2H, br m, NCH_2), 3.25 (2H, br m, NCH_2), 1.35 (12H, d, $^3J_{\text{HH}} = 6.7\text{ Hz}$, CHMe_2), 1.16–1.23 (38H, overlapping m, CHMe_2 and $\text{CH}_2(\text{CH}_2\text{N})_2$), 0.79 (1H, s, OH). $^{13}\text{C}\{^1\text{H}\}$ NMR (C_6D_6 , 101 MHz, 298 K): δ_{C} 148.1 ($\text{Ge}\{\text{C}(\text{CH})_4(\text{NO})\}$), 146.7 (*o*-C of Dipp), 146.5 (*o*-C of Dipp), 141.0 (*i*-C of Dipp), 136.1

(Ge{C(CH)₃CH(NO)}), 131.5 (Ge{C(CH)₂CHCH(NO)}), 129.0 (*p*-C of Dipp), 128.0 (*m*-C of Dipp), 127.2 (*m*-C of Dipp), 123.9 and 123.8 (Ge{CCH(CH)₃(NO)} and Ge{C(CH)₂CHCH(NO)}), 118.9 (N(CH)₂N of boryl ligand), 47.8 (NCH₂), 33.4 (CH₂(CH₂N)₂), 28.8 (CHMe₂), 28.5 (CHMe₂), 26.5 (CHMe₂), 26.0 (CHMe₂), 23.6 (CHMe₂), 22.6 (CHMe₂). ¹¹B NMR (C₆D₆, 128 MHz, 298 K): δ_B 24 (br s, boryl ligand).

X-ray Crystallography

Single-crystal X-ray diffraction data for all compounds (except (L¹)Sn) were collected on a Nonius KappaCCD diffractometer using Mo Kα radiation (λ = 0.71073 Å) or on an Oxford Diffraction Supernova diffractometer using mirror monochromated Cu Kα radiation (λ = 1.5418 Å) at 150 K. Crystals were selected under Paratone-N or perfluoropolyether oil, mounted on MiTeGen loops and quench-cooled using an Oxford Cryosystems open flow N₂ cooling device.²¹ Data collection and reduction were carried out using Collect and Denzo/Scalepack (Nonius KappaCCD)²² or the CrysAlisPro package (Oxford Diffraction Supernova).²³ Structures were subsequently solved using SHELXT²⁴ and refined on F² using the SHELXL 2018 package and the graphical interface Olex2 or X-Seed.^{25–27} The structure of (L¹)Ge was solved by Superflip,²⁸ and refined using full-matrix least-squares refinement with CRYSTALS.^{29–31} The structure of (L¹)Sn was solved ab initio from the integrated intensities using SHELXT,²⁴ and refined using full-matrix least-squares refinement with CRYSTALS.^{29–31} PLATON/SQUEEZE^{32,33} was used to model diffuse scattering in the void space. CCDC numbers: 1921772–1921780.

DFT Calculations

All computational work reported here utilized density functional theory (DFT), including geometry optimizations, and determination of the energies of the frontier orbitals of the tetrelenes, were performed using the Amsterdam Density Functional (ADF) 2014 software package. Calculations were performed using the Vosko-Wilk-Nusair local density approximation with exchange from Becke,³⁴ and correlation correction from Perdew.³⁵ Slater-type orbitals (STOs) were used for the triple zeta basis set with an additional set of polarization functions (TZP).³⁶ The full-electron basis set approximation was applied with no molecular symmetry. General numerical quality was good. Geometric details and molecular orbital energies were obtained after unrestricted geometry optimization.

Conflicts of interest

There are no conflicts to declare.

Acknowledgements

We acknowledge funding from the Oxford University Clarendon Scholarship Fund (LK); the EU 7th Framework Program, Marie Skłodowska-Curie actions (COFUND, Grant Agreement no. 267226) and Junta de Andalucía for a Talentia Postdoc (JC); the

EU 7th Framework Program, Marie Skłodowska-Curie actions (grant number PIEF-GA-2013-626441, EK); the Leverhulme Trust (grant number RP-2018-246, JH); the EPSRC (grant number EP/L025000/1, AP).

References

- For key early publications, see: (a) P.J. Davidson and M.F. Lappert, *J. Chem. Soc., Chem. Commun.*, 1973, 317; (b) D. H. Harris and M. F. Lappert, *J. Chem. Soc., Chem. Commun.*, 1974, 895; (c) M. J. S. Gynane, M. F. Lappert, S. J. Miles and P. P. Power, *J. Chem. Soc., Chem. Commun.*, 1976, 256; (d) D. E. Goldberg, D. H. Harris, M. F. Lappert and K. M. Thomas, *J. Chem. Soc., Chem. Commun.*, 1976, 261. See also: (e) M. F. Lappert, *J. Organomet. Chem.*, 1975, **100**, 139.
- See for example: (a) A. V. Protchenko, K. H. Birj Kumar, D. Dange, A. D. Schwarz, D. Vidovic, C. Jones, N. Kaltsoyannis, P. Mountford and S. Aldridge, *J. Am. Chem. Soc.*, 2012, **134**, 6500; (b) C. A. Caputo and P. P. Power, *Organometallics*, 2013, **32**, 2278; (c) Y. Peng, B. D. Ellis, X. Wang and P. P. Power, *J. Am. Chem. Soc.*, 2008, **130**, 12268; (d) A. Jana, C. Schulzke and H. W. Roesky, *J. Am. Chem. Soc.*, 2009, **131**, 4600; (e) A. Jana, I. Objartel, H. W. Roesky and D. Stalke, *Inorg. Chem.*, 2009, **48**, 798.
- (a) Y. Segawa, M. Yamashita, K. Nozaki, *Science* 2006, **314**, 113; (b) Y. Segawa, Y. Suzuki, M. Yamashita, K. Nozaki, *J. Am. Chem. Soc.* 2008, **130**, 16069; (c) M. Yamashita, Y. Suzuki, Y. Segawa, K. Nozaki, *Chem. Lett.* 2008, **37**, 802.
- For reviews of metal boryl chemistry see, for example: (a) G.J. Irvine, M.J.G. Lesley, T.B. Marder, N.C. Norman, C.R. Rice, E.G. Robins, W.R. Roper, G.R. Whittell, L.J. Wright, *Chem. Rev.* 1998, **98**, 2685; (b) D.L. Kays, S. Aldridge, *Struct. Bonding (Berlin)* 2008, **130** 29; (c) L. Dang, Z. Lin, T.B. Marder, *Chem. Commun.* 2009, 3987; (d) H. Braunschweig, R.D. Dewhurst, A. Schneider, *Chem. Rev.* 2010, **110**, 3924; (e) L. Weber, *Eur. J. Inorg. Chem.* 2017, **2017**, 3461.
- (a) L. M. A. Saleh, K. H. Birj Kumar, A. V. Protchenko, A. D. Schwarz, S. Aldridge, C. Jones, N. Kaltsoyannis, P. Mountford, *J. Am. Chem. Soc.* 2011, **133**, 3836; (b) A. V. Protchenko, K. H. Birj Kumar, D. Dange, A. D. Schwarz, D. Vidovic, C. Jones, N. Kaltsoyannis, P. Mountford, S. Aldridge, *J. Am. Chem. Soc.* 2012, **134**, 6500; (c) A. V. Protchenko, D. Dange, A. D. Schwarz, C. Y. Tang, N. Phillips, P. Mountford, C. Jones, S. Aldridge, *Chem. Commun.* 2014, **50**, 3841; (d) A. V. Protchenko, D. Dange, J. R. Harmer, C. Y. Tang, A. D. Schwarz, M. J. Kelly, N. Phillips, R. Tirfoin, K. H. Birj Kumar, C. Jones, N. Kaltsoyannis, P. Mountford, S. Aldridge, *Nature Chem.* 2014, **6**, 315; (e) A. V. Protchenko, D. Dange, M. P. Blake, A. D. Schwarz, C. Jones, P. Mountford, S. Aldridge, *J. Am. Chem. Soc.* 2014, **136**, 10902; (f) R. Frank, J. Howell, R. Tirfoin, D. Dange, C. Jones, D.M.P. Mingos, S. Aldridge, *J. Am. Chem. Soc.* 2014, **136**, 15730; (g) A. V. Protchenko, M. P. Blake, A. D. Schwarz, C. Jones, P. Mountford, S. Aldridge, *Organometallics* 2015, **34**, 2126; (h) R. Frank, J. Howell, J. Campos, R. Tirfoin, N. Phillips, S. Zahn, D.M.P. Mingos, S. Aldridge, *Angew. Chem., Int. Ed.* 2015, **54**, 9586; (i) A. V. Protchenko, J. I. Bates, L. M. A. Saleh, M. P. Blake, A. D. Schwarz, E. L. Kolychev, A. L. Thompson, C. Jones, P. Mountford, S. Aldridge, *J. Am. Chem. Soc.* 2016, **138**, 4555; (j) A. Rit, J. Campos, H. Niu, S. Aldridge, *Nature Chem.* 2016, **8**, 1022; (k) A. V. Protchenko, J. Urbano, J. A. B. Abdalla, J. Campos, D. Vidovic, A. D. Schwarz, M. P. Blake, P. Mountford, C. Jones, S. Aldridge, *Angew. Chem., Int. Ed.* 2017, **56**, 15098.
- (a) T. J. Hadlington, J. A. B. Abdalla, R. Tirfoin, S. Aldridge, C. Jones, *Chem. Commun.* 2016, **52**, 1717. See also: (b) B. A. Clough, S. Mellino, E. Clot, P. Mountford, *J. Am. Chem. Soc.* 2017, **139**, 11165; (c) B. A. Clough, S. Mellino, A. V. Protchenko, M. Slusarczyk, L. C. Stevenson, M. P. Blake, B. Xie,

- E. Clot, P. Mountford, *Inorg. Chem.* 2017, **56**, 10794; (d) (d) J. A. Kelly, M. Juckel, T. J. Hadlington, I. Fernández, G. Frenking, C. Jones, *Chem.-Eur. J.*, 2019, **25**, 2773.
- 7 Y. K. Loh, L. Ying, M. Á. Fuentes, D. C. H. Do and S. Aldridge, *Angew. Chem., Int. Ed.* 2019, **58**, 4847.
- 8 L. Kristinsdóttir, P. Vasko, H. Niu, E. L. Kolychev, J. Campos, M. Á. Fuentes, J. Hicks, A. L. Thompson, and S. Aldridge, *Chem.-Eur. J.*, 2019, **25**, 2556.
- 9 D. Herrmannsdorfer, M. Kaaz, O. Puntigam, J. Bender, M. Nieger, D. Gudat, *Eur. J. Inorg. Chem.* 2015, 4819.
- 10 B. Cordero, V. Gomez, A. E. Platero-Prats, M. Reves, J. Echeverria, E. Cremades, F. Barragan and S. Alvarez, *Dalton Trans.*, 2008, 2832.
- 11 R. W. Alder and M. E. Blake, *J. Phys. Chem. A*, 1999, **103**, 11200.
- 12 S. Halbert, C. Coperet, C. Raynaud, O. Eisenstein, *J. Am. Chem. Soc.*, 2016, **138**, 2261.
- 13 Y. Wang and J. Ma, *J. Organomet. Chem.* 2009, **694**, 2567.
- 14 M. Usher, A. V. Protchenko, A. Rit, J. Campos, E. L. Kolychev, R. Tirfoin, S. Aldridge, *Chem. Eur. J.*, 2016, **22**, 11685.
- 15 For related publications of heterocyclic germynes featuring electropositive *N*-substituents see, for example: (a) J. Böserle, G. Zhigulin, S. Ketkov, R. Jambor, A. Růžicka and L. Dostál, *Dalton Trans.*, 2018, **47**, 14880; (b) M. Vieth and R. Lisowsky, *Angew. Chem. Int. Ed. Engl.*, 1988, **27**, 1087; (c) J. Pfeiffer, W. Maringele, M. Noltemeyer and A. Meller, *Chem. Ber.*, 1989, **122**, 245; (d) S.M.I. Al-Rafia, P.A. Lummis, M.J. Ferguson, R. McDonald and E. Rivard, *Inorg. Chem.*, 2010, **49**, 9709; (e) S.K. Liew, S.M.I. Al-Rafia, J.T. Goettel, P.A. Lummis, S.M. McDonald, L.J. Miedema, M.J. Ferguson, R. McDonald and E. Rivard, *Inorg. Chem.*, 2012, **51**, 5471; (f) H. Arij, T. Amari, J. Kobayashi, K. Mochida and T. Kawashima, *Angew. Chem. Int. Ed.*, 2012, **51**, 6738; (g) D. Yang, J. Guo, H. Wu, Y. Ding and W. Zheng, *Dalton Trans.*, 2012, **41**, 2187; (h) P. Steiniger, G. Bendt, D. Bläser, C. Wölper and S. Schulz, *Chem. Commun.*, 2014, **50**, 15461; (i) J. Oetzel, N. Weyer, C. Bruhn, M. Leibold, B. Gerke, R. Pöttgen, M. Maier, R.F. Winter, M. Holthausen and U. Siemeling, *Chem.-Eur. J.*, 2017, **23**, 1187.
- 16 J. Kupp, M. Remko and P. von R. Schleyer, *J. Am. Chem. Soc.*, 1996, **118**, 5745.
- 17 See for example: (a) L. Li, T. Fukawa, T. Matsuo, D. Hashizume, H. Fueno, K. Tanaka and K. Tamao, *Nat. Chem.*, 2012, **4**, 361; (b) I. Alvarado-Beltran, A. Rosas-Sanchez, A. Baceiredo, N. Saffon-Merceron, V. Branchadell and T. Kato, *Angew. Chem. Int. Ed.*, 2017, **56**, 10481; (c) A. Rosas-Sanchez, I. Alvarado-Beltran, A. Baceiredo, N. Saffon-Merceron, S. Massou, D. Hashizume, V. Branchadell and T. Kato, *Angew. Chem. Int. Ed.*, 2017, **56**, 15916; (d) D. Wendel, D. Reiter, A. Porzelt, J. Altmann, S. Inoue and B. Rieger, *J. Am. Chem. Soc.* 2017, **139**, 17193; (e) R. Kobayashi, S. Ishida and T. Iwamoto, *Angew. Chem. Int. Ed.*, in press (DOI: 10.1002/anie.201905198).
- 18 M. Veith and A. Rammo, *Z. Anorg. Allg. Chem.*, 1997, **623**, 861.
- 19 A. B. Pangborn, M. A. Giardello, R. H. Grubbs, R. K. Rosen and F. J. Timmers, *Organometallics*, 1996, **15**, 1518.
- 20 P. J. Bailey, R. A. Coxall, C. M. Dick, S. Fabre, L. C. Henderson, C. Herber, S. T. Liddle, D. Loroño-Gonzalez, A. Parkin and S. Parsons, *Chem. Eur. J.*, 2003, **9**, 4820.
- 21 J. Cosier, A. M. Glazer, *J. Appl. Cryst.* 1986, **19**, 105.
- 22 Z. Otwinowski, W. Minor, *Processing of X-ray Diffraction Data Collected in Oscillation Mode, Methods Enzymol.* 1997, **276**, Eds C. W. Carter, R. M. Sweet, Academic Press.
- 23 CrysAlisPro v.1.171.35.8 (Agilent Technologies, 2011).
- 24 G. M. Sheldrick, G. M. *Acta Cryst.* 2015, **A71**, 3.
- 25 G. M. Sheldrick, *Acta Cryst.* 2015, **C71**, 3.
- 26 O. V. Dolomanov, L. J. Bourhis, R. J. Gildea, J. A. K. Howard, H. Puschmann, *J. Appl. Crystallogr.* 2009, **42**, 339.
- 27 L. J. Barbour, *J. Supramol. Chem.* 2001, **1**, 189.
- 28 L. Palatinus, and G. Chapuis, *J. Appl. Cryst.*, 2007, **40**, 786.
- 29 P. W. Betteridge, J. R. Carruthers, R. I. Cooper, K. Prout, D. J. Watkin, *J. Appl. Cryst.* 2003, **36**, 1487.
- 30 P. Parois, R. I. Cooper, A. L. Thompson, *Chem. Cent. J.* 2015, **9**, 30.
- 31 R. I. Cooper, A. L. Thompson, D. J. Watkin, *J. Appl. Cryst.* 2010, **43**, 1100.
- 32 A. Spek, *J. Appl. Cryst.* 2003, **36**, 7.
- 33 P. van der Sluis, A. L. Spek, *Acta Cryst.* 1990, **A46**, 194.
- 34 A. D. Becke, *Phys. Rev. A*, 1988, **38**, 3098.
- 35 J. P. Perdew, *Phys. Rev. B*, 1986, **33**, 8822.
- 36 S. Grimme, J. Antony, S. Ehrlich, H. Krieg, *J. Chem. Phys.* 2010, **132**, 154104; (b) S. Grimme, S. Ehrlich, L. Goerigk, *J. Comput. Chem.* 2011, **32**, 1456.